Origin of two maxima in specific heat in enthalpy relaxation under thermal history composed of cooling, annealing, and heating

Waki Sakatsuji,[1,*] Takashi Konishi,[2] and Yoshihisa Miyamoto[2]

[1]*Division of Physics and Astronomy, Graduate School of Science, Kyoto University, Kyoto, Japan*
[2]*Graduate School of Human and Environmental Studies, Kyoto University, Kyoto, Japan*

The origin of two maxima in specific heat observed at the higher and the lower temperatures in the glass-transition region in the heating process has been studied for polymethyl methacrylate and polyvinyl chloride using differential scanning calorimetry, and the calculation was done using the phenomenological model equation under a thermal history of the typical annealing experiment composed of cooling, annealing, and heating. The higher maximum is observed above the glass-transition temperature, and it remains almost unchanged independent of annealing time t_a, while the lower one is observed above an annealing temperature T_a and shifts toward the higher one, increasing its magnitude with t_a. The analysis by the phenomenological model equation proposed in order to interpret the memory effect in the glassy state clarifies that under a typical annealing history, two maxima in specific heat essentially appear. The shift of the lower maximum toward higher temperatures from above T_a is caused by an increase in the amount of relaxation during annealing with t_a. The annealing temperature and the amount of relaxation during annealing play a major role in the determination of the number of maxima in the specific heat.

I. INTRODUCTION

When glass-forming liquid is heated from the glassy state, the overshoot of specific heat against temperature is observed in the glass-transition region, and this phenomenon is called enthalpy relaxation. The magnitude and the temperature of the specific-heat peak decrease or increase depending on the thermal history. Conventionally, the memory effect in enthalpy relaxation has been analyzed using the phenomenological model, including the fictive temperature [1], which depends not only on temperature but also on instantaneous structures such as the Tool-Narayanaswamy-Moynihan (TNM) model [1–3] and the Kovacs-Aklonis-Hutchinson-Ramos (KAHR) model [4]. These models introduced the nonlinear parameter that partitions the actual temperature and the fictive temperature, and they described the memory effect. The models are widely used, and quantitative agreements with the experimental results have been reported. Gómez and Monleón have proposed that the state reached after sufficiently long-time annealing is not equal to the state extrapolated from the equilibrium liquid state at a high temperature [5]. Recently, some studies have discussed the existence of an aging plateau [6–9] by focusing on the total enthalpy decay after long-time aging. The aging plateau is the state reached at very long-time aging, and in this state the system has higher enthalpy than the extrapolated enthalpy from the equilibrium liquid state. Two-step relaxation after the aging plateau has also been reported in the enthalpy relaxation in polystyrene (PS) [8] and chalcogenide glass [7]. Multiple relaxations are observed in the Brillouin frequency shift of glycerol [10]. Contrary to these studies, Koh and Simon have reported that the aging plateau does not exist in PS with a broad distribution of molecular weights [11]. The existence of the aging plateau may depend on the distribution of molecular weights. These studies focus

on the total enthalpy decay, and they do not take into account the memory effect in the enthalpy relaxation.

We have studied the annealing effects on the enthalpy relaxation in PS [12] on the basis of a comparison between the experimental results and the calculated ones by using the phenomenological model equation proposed in order to examine the memory effect on viscoelasticity in the glassy state [13]. The analysis by our model is based on the calculation with parameters experimentally obtained or with physically clear ones. Our model is an extension of the linear-response theory to nonlinear phenomena, and it allows us to examine the history of which point in time in the past affects the physical properties at the present time.

Polystyrene is a typical glassy polymer, and it is said to show only one maximum in specific heat under a typical thermal history of the annealing experiment, as shown in Fig. 1: cooling from the equilibrium liquid state to an annealing temperature at a constant rate, isothermal annealing, further cooling at the same rate to the glassy state, and reheating to the liquid state. Under such a typical thermal history, some glassy polymers, such as polymethyl methacrylate (PMMA) and polyvinyl chloride (PVC), show two maxima in specific heat in the heating process [14–18].

The β relaxation is observed as well as the α relaxation in the dielectric or the mechanical measurement in PMMA and PVC [19–23], but not in the calorimetry [24]. We have studied the effects of annealing on the enthalpy relaxation in PMMA, and we reported part of the results and the analyses [18]. It turned out that two relaxations are not always necessary for two maxima in specific heat since the parameter fitting or the calculation by the model with only one relaxation has reproduced two maxima in the specific heat [14,18].

The purpose of the present study is to clarify the origin of two maxima in specific heat under the thermal history of a typical annealing experiment. In addition to PMMA, PVC is also used as a sample. We first explain the model used in this paper in Sec. II. Next we outline the measurements of
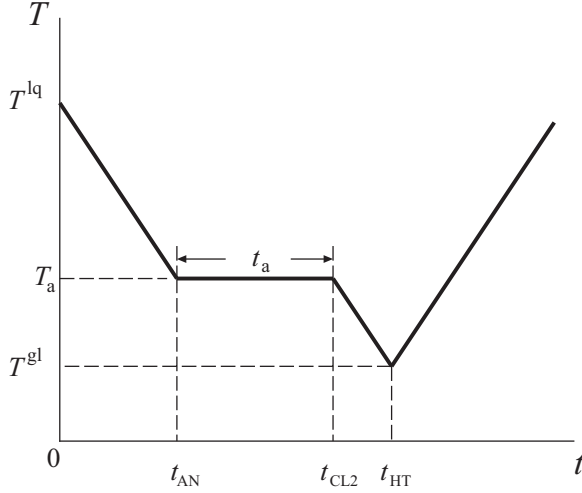
*sakatsuji.waki.5n@kyoto-u.ac.jp

FIG. 1. Schematic diagram of the thermal history in the annealing experiments.

basic relaxation parameters and the annealing experiments in Sec. III, and we show the results of these experiments in Secs. IV A and IV B. In Sec. IV C, three methods of calculations (1, 2, and 3) are explained. In calculation 1, which is important for the purpose of this paper, the relaxation time is assumed to be the equilibrium one obtained by extrapolation from the equilibrium liquid state over the entire temperature range, including the glassy state below T_g. Section IV D is the main part of this paper, and we discuss qualitatively the origin of two maxima in specific heat based on calculation 1. In Sec. IV E we perform calculations 2 and 3 in order to examine a quantitative agreement, and finally we comment on the possibility of two maxima in PS.

II. PHENOMENOLOGICAL MODEL

The model used in this paper is the same one that was used in previous studies. The details are given in previous papers [12,18]. The evolution of entropy under a given thermal history is calculated by the phenomenological model equation,

$$S(t) = S^{eq}[T(t)] - \int_{-\infty}^{t} \overline{\Delta\chi}[T(t),T(t')][T(t) - T(t')]$$

$$\times \frac{\partial\phi[\tilde{t}(t,t')]}{\partial t'} dt', \tag{1}$$

$$\overline{\Delta\chi}[T(t),T(t')] = \frac{1}{T(t) - T(t')} \int_{T(t')}^{T(t)} \frac{\Delta C_p(T'')}{T''} dT'', \tag{2}$$

$$\tilde{t}(t,t') \equiv \int_{t'}^{t} \frac{du}{\tau(u)}, \tag{3}$$

where $S^{eq}(T)$ is the entropy in the equilibrium liquid state, $\overline{\Delta\chi}[T(t),T(t')]$ is the susceptibility for entropy, $\Delta C_p(T)$ is the difference between the liquid and the glassy specific heat [$C_p^0(T)$ and $C_p^\infty(T)$, respectively], and $\phi(t)$ is the normalized relaxation function. The intrinsic time lapse, or the reduced time $\tilde{t}(t,t')$, gives the time lapse between t' and t measured with the instantaneous relaxation time, $\tau(u)$.
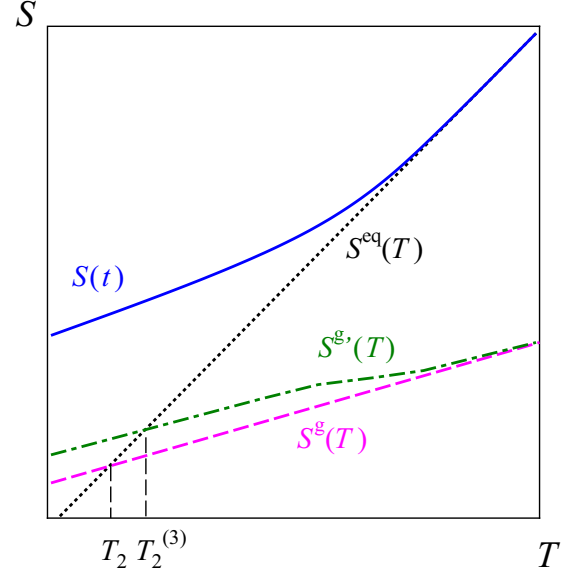

FIG. 2. Schematic graph of entropy against temperature. The solid, dotted, dashed, and dashed-dotted lines represent the instantaneous entropy $S(t)$, the liquid entropy $S^{eq}(T)$, the hypothetical glassy entropy $S^g(T)$ defined by Eq. (6), and the modified glassy entropy $S^{g'}(T)$ defined by Eq. (7), respectively. At a temperature T_2, S^g is equal to S^{eq}.

For the relaxation time τ in $\tilde{t}(t,t')$ in Eq. (3), we assume that the relaxation time obeys the Adam-Gibbs theory [25] in the out-of-equilibrium glassy state as well as in the equilibrium liquid state [26,27], and it is determined by

$$\tau = \tau_\infty \exp\left[\frac{A}{T S_c}\right], \tag{4}$$

$$S_c = S - S^g(T), \tag{5}$$

$$S^g(T) = S^{eq}(T_2) + \int_{T_2}^{T} \frac{C_p^\infty(T')}{T'} dT', \tag{6}$$

where τ_∞ and A are constants, S_c is the configurational entropy, and $S^{eq}(T)$ and $S^g(T)$ are the liquid entropy and the hypothetical glassy entropy, respectively, schematically shown in Fig. 2. At a temperature T_2, S^g is equal to S^{eq}. The calculated results are compared with the results of the annealing experiments, and we discuss the origin of two maxima in specific heat in the enthalpy relaxation.

III. EXPERIMENT

A. Material and differential scanning calorimetry

The materials used in this study were PMMA with a molecular weight $M_w = 75\,000$ and PVC with $M_w = 275\,000$ purchased from Scientific Polymer Products. No trace of crystallinity in PVC has been observed by wide-angle x-ray diffraction before and after the experiments. The glass-transition temperature T_g of PMMA and PVC defined by the equal area method [3] is 105.0 and 85.0 °C at the cooling rate of 9.7 K/min, respectively. The DSC measurement was carried out by DSC-60 (Shimadzu Corp.). In the glassy

state, two sources of entropy exist: one originates from the heat exchanged and the other from the irreversibility of the processes taking place in the nonequilibrium system [28], and in the case of mild variation of T_f, the entropy irreversibly produced is negligible [29]. The apparent specific heat, C_p, is defined in this paper by $C_p = \dot{Q}/w\dot{T}$, where $\dot{Q}$ is the heat flux observed in the DSC measurement, w is the weight of the sample, and $\dot{T}$ is the time derivative of temperature T. The entropy in this paper is determined from thus defined apparent C_p. In all the experiments, the memories of the samples were erased by annealing at a temperature in the equilibrium liquid state $T^{lq} = 200\,°C$ for PMMA and $170\,°C$ for PVC for 1 min.

B. Complex specific-heat measurements

The sample of about 4.4 mg and 0.2 mm in thickness for PMMA and the powdery sample of about 4.3 mg for PVC were cooled to a temperature T_0 in the range from 40 to $160\,°C$ for PMMA and from 30 to $150\,°C$ for PVC at 9.7 K/min and kept for 3 min. Then the sample underwent the sinusoidal temperature variation centered at T_0 with an amplitude of 0.5 K and a period P in the range from 20 to 200 s.

C. Annealing experiments

In the measurements of the dependence of enthalpy relaxation on the annealing conditions, the samples from 4 to 16 mg were employed. The results of the sample of 7 mg in weight for PMMA and of 11 mg for PVC are shown as the annealing experimental results; no systematic variation in the heat flow with the sample weight was observed.

Figure 1 shows the thermal history of the annealing experiment. In the annealing experiments, the sample was cooled from a high temperature T^{lq} to an annealing temperature T_a in the range from 60 to $115\,°C$ for PMMA and from 50 to $85\,°C$ for PVC, annealed for t_a in the range from 1 to 3×10^3 min, further cooled to a temperature T^{gl} well below T_g and then heated to T^{lq} followed by the second run; T^{gl} was $30\,°C$ for PMMA and $20\,°C$ for PVC. The second run comprised the cooling from T^{lq} to T^{gl} and heating to $180\,°C$ for PMMA or $160\,°C$ for PVC. The results of the second run were used for the baseline correction and the examination of the sample degradation. The heating and the cooling rates were all 9.7 K/min. All the thermal treatments were carried out in the calorimeter.

IV. RESULTS AND DISCUSSION

A. Relaxation parameters

The results of the complex specific-heat measurements for PVC are shown in Figs. 3, 4, and 5. We obtained the temperature dependence of the liquid and the glassy specific heat, $C_p^0(T)$ and $C_p^\infty(T)$, from the real part of the specific heat at high and low temperatures, respectively. We assume that $C_p^0(T)$ and $C_p^\infty(T)$ are linear in T in the temperature range of the measurement, i.e., $C_p^0(T) = a^\ell T + b^\ell$ and $C_p^\infty(T) = a^g T + b^g$, and we obtained coefficients of C_p^0 and C_p^∞. The relaxation time $\tau(T)$ was obtained from the peak temperatures of the imaginary part of specific heat, T_α in Fig. 3, by $\tau(T_\alpha) = P/2\pi$ and shown in Fig. 4, where P is the period of the temperature
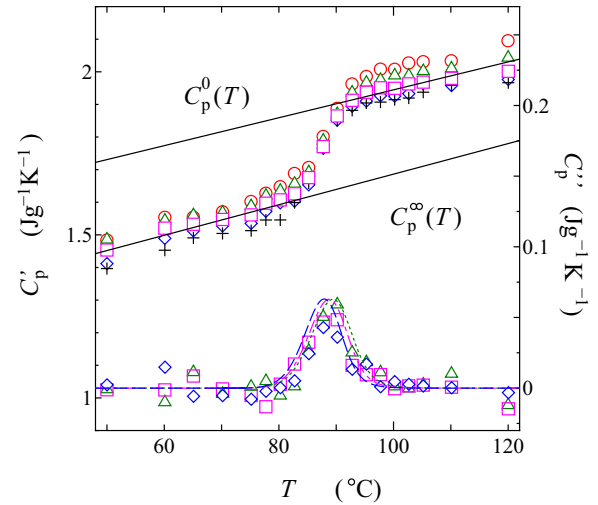

FIG. 3. Temperature dependence of the real (upper data) and the imaginary parts (lower data) of specific heat for PVC. The symbols represent the experimental data. $\bigcirc$: $P = 20$ s, $\triangle$: 30 s, $\square$: 50 s, $\diamond$: 100 s, $+$: 200 s. The solid lines represent C_p^0 (upper) and C_p^∞ (lower), respectively. The dotted, dashed, and dashed-dotted curves represent C_p'' calculated for $P = 30$, 50, and 100 s, respectively.

modulation. The temperature dependence of relaxation time is assumed to be described by the Adam-Gibbs equation, and the least-squares fitting by Eq. (4) with $S_c(T) = S^{eq}(T) - S^g(T)$ gives the parameters $\tau_\infty = (8.4 \pm 3.9) \times 10^{-12}$ s, $A = 284.32 \pm 0.04$ J g^{-1}, and $T_2 = 325.8 \pm 0.6$ K. The complex specific heat normalized by $C_p^\infty(T)$ and $\Delta C_p(T)$, $C_p^{N\,*}(\omega\tau)$, is shown in Fig. 5, where $\Delta C_p(T)$ is the difference
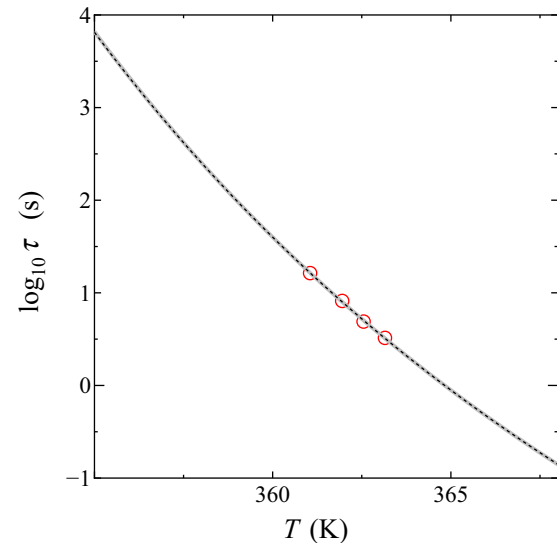

FIG. 4. Temperature dependence of the relaxation time for PVC. Open circles represent the experimental results. The relaxation time obtained from C_p'' for $P = 200$ s for PVC is not shown in the figure. The solid curve represents Eq. (4) with $S_c(T) = S^{eq}(T) - S^g(T)$, $\tau_\infty = 8.40 \times 10^{-12}$ s, $A = 284$ J g^{-1}, and $T_2 = 326$ K, and the dotted curve represents Eq. (4) with $S_c(T) = S^{eq}(T) - S^{g\prime}(T)$, $\tau_\infty^{(3)} = 4.08 \times 10^{-12}$ s, $A^{(3)} = 343$ J g^{-1}, and $T_2^{(3)} = 324$ K.
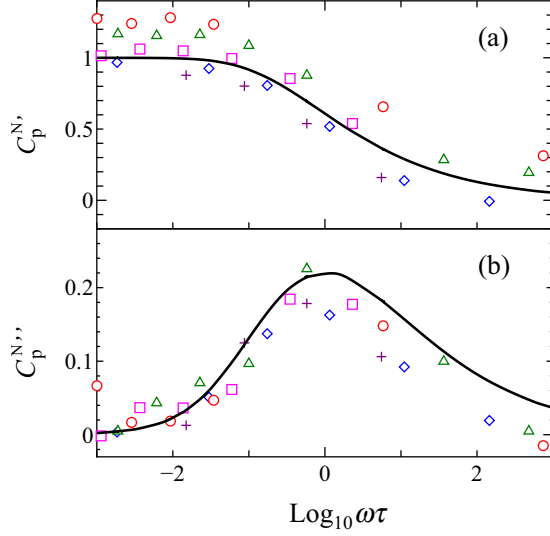
FIG. 5. (a) Real and (b) imaginary parts of normalized specific heat for PVC. $\bigcirc$: $P = 20$ s, $\triangle$: 30 s, $\square$: 50 s, $\diamondsuit$: 100 s, and $+$: 200 s. The solid curves represent the calculated ones by Fourier transform of $1 - \phi(t/\tau_{\mathrm{KWW}})$.

FIG. 6. Specific heat against temperature in the heating process after annealing for 10^3 min at T_{a} in the range from 49.8 to 85.1 °C for PVC. The symbols represent the experimental data; $\bullet$: unannealed data, $\bigcirc$: $T_{\mathrm{a}} = 49.8$ °C, $\square$: 55.0 °C, $\triangle$: 59.7 °C, $\diamondsuit$: 65.2 °C, $\triangledown$: 70.2 °C, $\triangleright$: 75.3 °C, $\triangleleft$: 80.5 °C, and $+$: 85.1 °C. The down and the up arrows represent the lower and the higher maxima in specific heat, respectively. The numbers in the figure represent the annealing temperature in °C.

between $C_{\mathrm{p}}^0(T)$ and $C_{\mathrm{p}}^{\infty}(T)$. The relaxation function was approximated by the KWW function [30] with a relaxation time, τ_{KWW}, proportional to the experimental τ, and an exponent β. The complex specific heat was calculated by the Fourier transform of $1 - \phi(t/\tau_{\mathrm{KWW}})$ and compared with the data in Fig. 5. The best-fit values of β and τ_{KWW} thus obtained were $\beta = 0.40 \pm 0.08$ and $\tau_{\mathrm{KWW}} = (0.69 \pm 0.26)\tau$. The value of β for PVC obtained by our thermal measurement is larger than that by the dielectric measurement ($\beta = 0.23 \pm 0.03$ [31]). The parameters obtained by the measurements in Sec. IV A for PMMA and PVC are summarized together with the results for PS for comparison in Table I.

B. Dependence of specific heat on annealing conditions

Since the purpose of this paper is to discuss the origin of two maxima in specific heat, we examine the experimental conditions under which two maxima in specific heat are observed, and we mainly show the experimental results in the case of two maxima. The results of annealing measurements are shown in Figs. 6, 7(a), 7(b), and 8. Figure 6 shows the temperature dependence of specific heat in the heating process
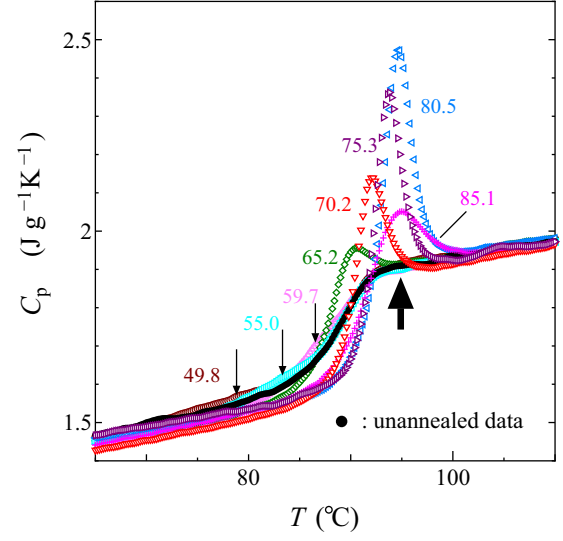
at 9.7 K/min after annealing at T_{a} in the range from 49.8 to 85.1 °C for 10^3 min for PVC. At $T_{\mathrm{a}} = 49.8$, 55.0, and 59.7 °C, two maxima in specific heat are observed. *When two maxima in specific heat are observed*, we call, for convenience, the maximum in specific heat observed at a lower temperature the *lower maximum* in specific heat, and that observed at a higher temperature the *higher maximum* in specific heat. In the case of PVC, the naming of the higher "maximum" may not be proper, and this should be described as a "kink" rather than a maximum. However, for convenience we call this kink a "maximum" in order to be in contrast with the lower maximum because in the preliminary measurements of the ramping rate dependence, the kink in specific heat grows into a conspicuous maximum with decreasing cooling rate and/or increasing heating rate.

The magnitude and the temperature of the lower maximum in specific heat, $C_{\mathrm{p\,max}}^{\mathrm{L}}(T_{\mathrm{a}}, t_{\mathrm{a}})$ and $T_{\mathrm{max}}^{\mathrm{L}}(T_{\mathrm{a}}, t_{\mathrm{a}})$, respectively, increase with annealing temperature T_{a}, while those of the

TABLE I. Parameters obtained by the temperature-modulated measurements for PS, PMMA, and PVC.

Sample	a^{ℓ} (J g^{-1} K^{-2})	b^{ℓ} (J g^{-1} K^{-1})	a^{g} (J g^{-1} K^{-2})	b^{g} (J g^{-1} K^{-1})
PS [12]	3.7×10^{-3}	6.1×10^{-1}	4.1×10^{-3}	9.0×10^{-2}
PMMA [18]	5.2×10^{-3}	1.6×10^{-1}	6.0×10^{-3}	-4.6×10^{-2}
PVC	4.3×10^{-3}	3.5×10^{-1}	4.7×10^{-3}	-6.3×10^{-2}

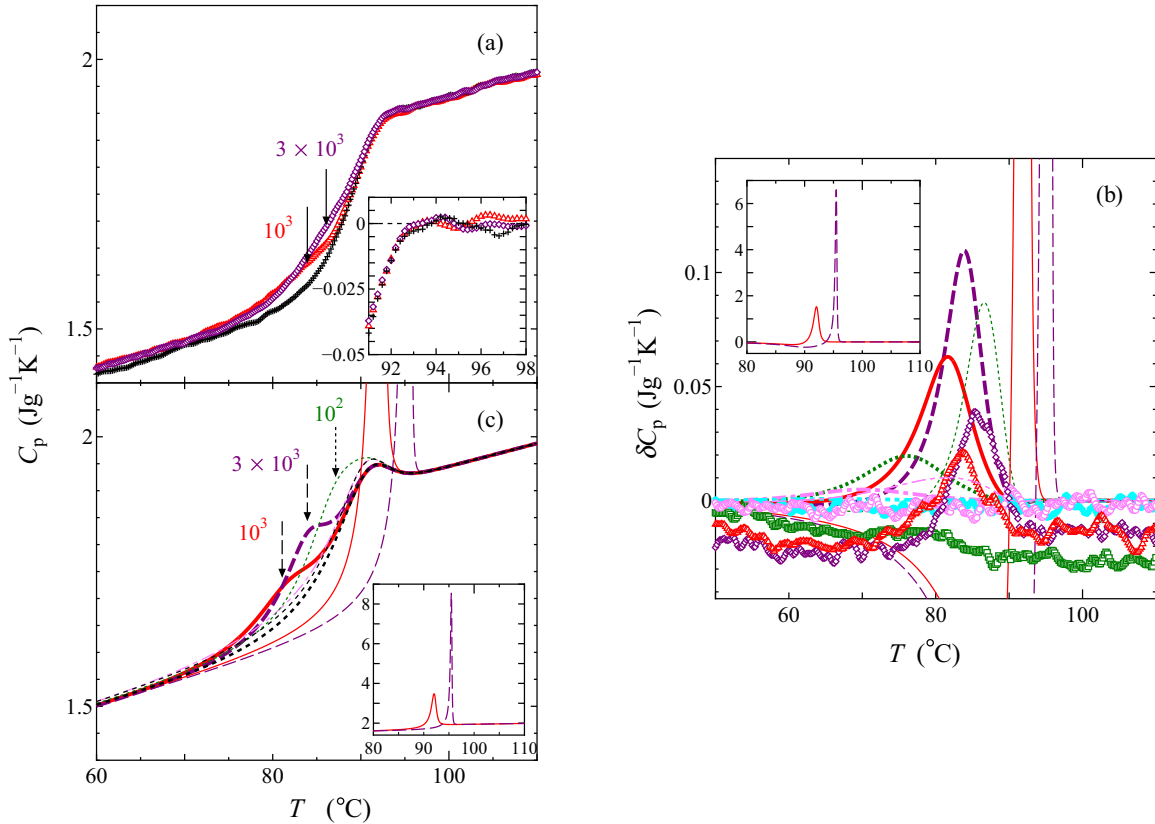| Sample	τ_{∞} (s)	A (J g^{-1})	T_2 (K)	β
PS [12]	1.28×10^{-8}	333	336	0.62 ± 0.09
PMMA [18]	1.88×10^{-4}	99.1	359	0.34 ± 0.06
PVC	8.40×10^{-12}	284	326	0.40 ± 0.08

FIG. 7. Specific heat in the heating process after annealing at $T_a = 55.0\,^\circ$C for t_a in the range from 1 to 3×10^3 min. (a) The experimental C_p for unannealed results and for $t_a = 10^3$ and 3×10^3 min for PVC. The excess specific heat is shown in the inset in (a). (b) δC_p for the experimental results and the results by the calculations 2 (thin) and 3 (thick) for t_a in the range from 1 to 3×10^3 min. (c) The results by the calculations 2 (thin) and 3 (thick). The plots of δC_p and C_p by the calculation 2 for $t_a = 10^3$ and 3×10^3 min are shown in the insets in (b) and (c), respectively. The shapes of the symbols represent t_a, $\bullet$: $t_a = 1$ min, $\bigcirc$: $t_a = 10$ min, $\square$: $t_a = 10^2$ min, $\triangle$: $t_a = 10^3$ min, and $\diamondsuit$: $t_a = 3 \times 10^3$ min, and the crossed symbol represents the unannealed data. The dashed-two dotted, dashed-dotted, dotted, solid, dashed, and short dashed curves in (b) and (c) are $t_a = 1$, 10, 10^2, 10^3, and 3×10^3 min, and unannealed data, respectively. The solid, dotted, and dashed down-arrows represent the lower maxima in specific heat of the experimental results of the calculations 2 and 3, respectively. The numbers in the figure represent the annealing time in minutes.

higher maximum, $C_{p\,max}^H(T_a, t_a)$ and $T_{max}^H(T_a, t_a)$, respectively, remain unchanged with T_a. T_{max}^L is determined by the maximum temperature of δC_p defined by the difference between the annealed C_p and the unannealed one, and $C_{p\,max}^L$ is $C_p(T = T_{max}^L)$. T_{max}^H is determined by the maximum temperature of the excess specific heat defined by $C_p - C_p^0$, and $C_{p\,max}^H$ is $C_p(T = T_{max}^H)$. At $T_a \geqslant 65.2\,^\circ$C, only one maximum in specific heat is observed. *When only one maximum is observed*, we call the one simply *the maximum* in specific heat, and the magnitude and the temperature of the maximum in specific heat, $C_{p\,max}^{(1)}$ and $T_{max}^{(1)}$, respectively, are determined in the same way as the higher maximum. $C_{p\,max}^{(1)}$ increases with T_a for $T_a \leqslant 80.5\,^\circ$C and decreases for $T_a > 80.5\,^\circ$C, and $T_{max}^{(1)}$ increases with T_a.

Figure 7(a) shows the annealing time dependence of the enthalpy relaxation for PVC. The specific heat against temperature in the heating process is shown for $T_a = 55.0\,^\circ$C and t_a of 10^3 and 3×10^3 min in the figure as examples of the case in which two maxima in specific heat are observed. The black crossed symbols represent the unannealed data. The excess specific heat is shown in the inset of Fig. 7(a).

The symbols in Fig. 7(b) show δC_p for $t_a = (1–3) \times 10^3$ min. Figure 7(b) shows that a discernible maximum is not observed at $t_a \leqslant 10^2$ min while the maxima in δC_p are clearly observed at $t_a \geqslant 10^3$ min. The magnitude and the temperature at a maximum in δC_p, corresponding to $C_{p\,max}^L$ and T_{max}^L, respectively, increase with t_a, while $C_{p\,max}^H$ and T_{max}^H remain unchanged with t_a. The similar results have been obtained for PMMA at an annealing temperature, e.g., $T_a = 80.1\,^\circ$C [18].

The symbols in Figs. 8(a) and 8(b) show the annealing temperature dependence of $C_{p\,max}^H$, $C_{p\,max}^L$, and $C_{p\,max}^{(1)}$, and of T_{max}^H, T_{max}^L, and $T_{max}^{(1)}$, respectively, for $t_a = 10^2$, 10^3, and 3×10^3 min for PMMA (left) and for $t_a = 10^2$ and 10^3 min for PVC (right). Figure 8 shows that for a given t_a, two maxima in specific heat are observed within an annealing temperature range. At high annealing temperatures, only one maximum in specific heat is observed. At very low annealing temperatures, the lower maximum in specific heat cannot be determined within the experimental accuracy and hence only one maximum is observed. Similarly for a very short annealing time, the lower maximum cannot be determined. At high annealing temperatures, $C_{p\,max}^{(1)}$ increases at first and then decreases with T_a, and $T_{max}^{(1)}$ increases with T_a. The upper limit
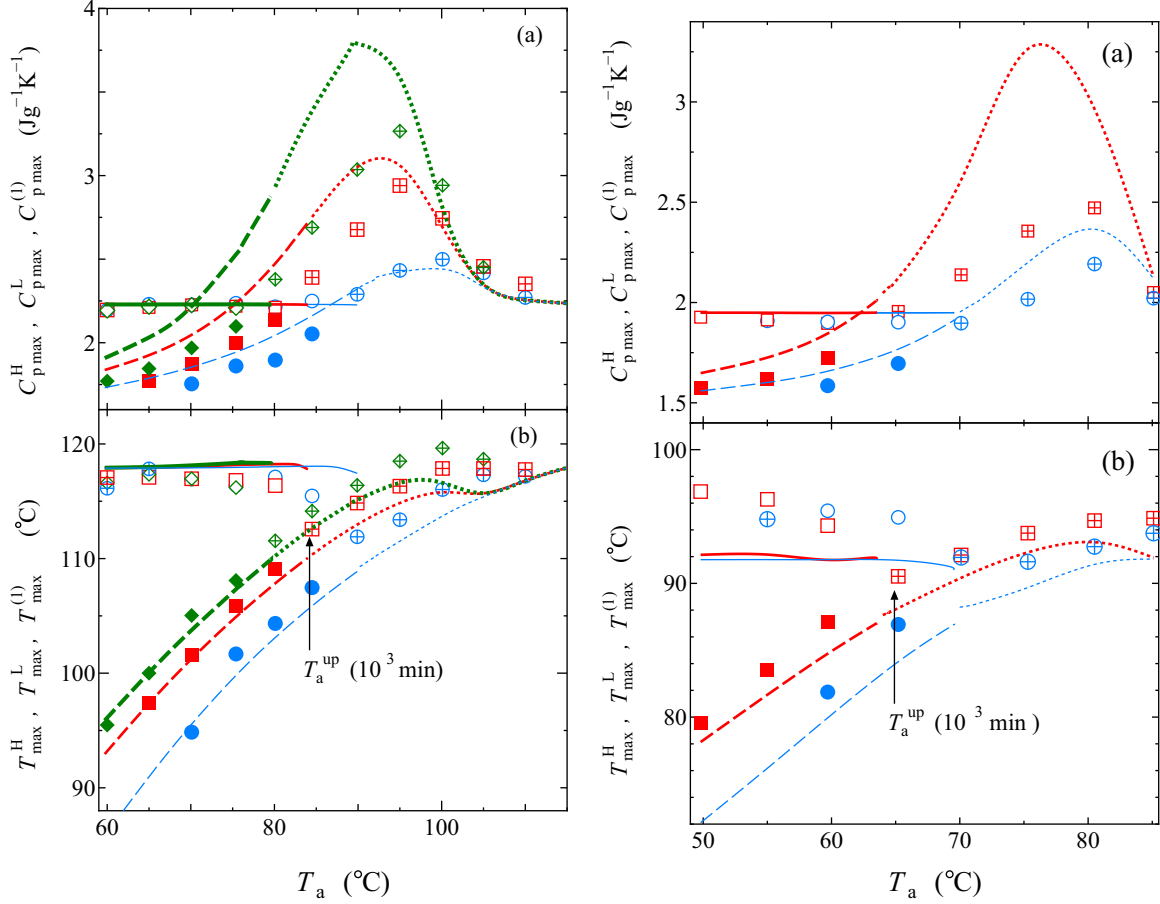
FIG. 8. Annealing temperature dependence of (a) $C_{p\,max}^{L}$, $C_{p\,max}^{H}$, and $C_{p\,max}^{(1)}$; and (b) T_{max}^{L}, T_{max}^{H}, and $T_{max}^{(1)}$, respectively, for PMMA (left) and PVC (right). The symbols represent the results of annealing experiments and the curves the results by calculation 3. The filled symbols represent the magnitude and the temperature of lower maximum in specific heat, $C_{p\,max}^{L}$ and T_{max}^{L}. The open and crossed symbols represent those of higher maximum, $C_{p\,max}^{H}$ and T_{max}^{H}, and those of the maximum in the case of only one maximum, $C_{p\,max}^{(1)}$ and $T_{max}^{(1)}$, respectively. The shapes of symbols represent the annealing time are as follow: $\circ$: $t_a = 10^2$, $\square$: 10^3, and $\diamond$: 3×10^3 min. The line types represent the type of maximum in specific heat; dashed: $C_{p\,max}^{L}$ and T_{max}^{L}, solid: $C_{p\,max}^{H}$ and T_{max}^{H}, and dotted: $C_{p\,max}^{(1)}$ and $T_{max}^{(1)}$. The linewidth represents the annealing time; thin: $t_a = 10^2$, medium: $t_a = 10^3$, and thick: $t_a = 3 \times 10^3$ min, respectively.

of the annealing temperature where two maxima in specific heat are observed, T_a^{up}, decreases with annealing time.

The experimental results for the enthalpy relaxation in PMMA and PVC in the case of two maxima are summarized as follows. For a given t_a, for $T_a < T_a^{up}$, two maxima in specific heat are observed and $C_{p\,max}^{L}$ and T_{max}^{L} increase with T_a while $C_{p\,max}^{H}$ and T_{max}^{H} are almost unchanged independent of T_a. For an annealing temperature where two maxima in specific heat are observed, $C_{p\,max}^{L}$ and T_{max}^{L} increase while $C_{p\,max}^{H}$ and T_{max}^{H} are almost unchanged with increasing t_a

C. Calculation by the phenomenological model equation

The specific heat under a given thermal history is calculated with the relaxation parameters experimentally obtained in the following three methods according to the definition of the configurational entropy S_c. The details of the calculations are given in previous papers [12,18].

Calculation 1. The configurational entropy is assumed to be given by $S_c(T) = S^{eq}(T) - S^g(T)$. Hence the relaxation time is an equilibrium one at a temperature lower than T_g, as shown

in Fig. 4 and determined by the instantaneous temperature, i.e., $\tau[T(t)] = \tau^{eq}[T(t)]$.

Calculation 2. The configurational entropy at time t is assumed to be given by $S_c(t) = S(t) - S^g[T(t)]$ in terms of the instantaneous entropy $S(t)$. The relaxation time varies with cooling below T_g and with annealing time through $S(t)$.

In calculation 1, the relaxation time does not vary during annealing, that is, the entropy relaxes with a constant relaxation time determined by T_a toward equilibrium during isothermal annealing. In contrast, in calculation 2, the relaxation time varies during annealing through the decrease in $S(t)$, that is, the rate of relaxation to equilibrium varies with time even during isothermal annealing. These calculations are identical to the model used in Ref. [15] in that the relaxation time below T_g is described by extending the Adam and Gibbs equation to the glassy state. In these two calculations in the present paper the parameters only experimentally obtained are employed.

Calculation 3. A better agreement with the experimental results is examined by taking account of the additional contribution of the specific heat, $\Delta C(T)$, to the glassy entropy,

$S^{\mathrm{g}}(T)$, on the basis of the free-energy landscape (FEL) theory [32–34]. These studies suggest that the configurational entropy is not always given by Eq. (5), but $S^{\mathrm{g}}(T)$ includes an additional component originating from the temperature dependence of FEL and changes stepwise presumably in the glass-transition region. The glassy entropy taking into account $\Delta C(T)$, $S^{\mathrm{g}\prime}(T)$, is given by

$$S^{\mathrm{g}\prime}(T) = S^{\mathrm{eq}}\big(T_2^{(3)}\big) + \int_{T_2^{(3)}}^{T} \frac{C_{\mathrm{p}}^{\infty}(T') + \Delta C(T')}{T'}dT', \quad (7)$$

$$\Delta C(T) = \sqrt{\frac{2}{\pi}}\,\Delta\chi_{\mathrm{F}}\,T\,\exp\left[-\frac{(T - T_{\mathrm{F}})^2}{2\sigma_{\mathrm{F}}^2}\right], \quad (8)$$

where the simplest functional form of $\Delta C(T)$ is assumed so that $S^{\mathrm{g}\prime}$ shows the stepwise change in the glass-transition region as shown in Fig. 2 by the dash-dotted curve, and $\Delta\chi_{\mathrm{F}}$, σ_{F}, and T_{F} are the constant parameters independent of temperature and the experimental condition. The configurational entropy is given by $S_{\mathrm{c}}(t) = S(t) - S^{\mathrm{g}\prime}[T(t)]$, and the relaxation time is given by Eq. (4) with this configurational entropy.

D. Results and discussion based on calculation 1

Two maxima in specific heat are reproduced qualitatively by all the methods of the calculations, even by calculation 1, the simplest method in which the variation in the relaxation time during annealing is not considered.

We focus on the case of the two maxima in specific heat in this paper. We first show the results by calculation 1 in the case of two maxima in specific heat, and then we discuss the origin of two maxima in specific heat based on calculation 1.

In calculation 1, the range of annealing temperature where two maxima in specific heat are observed does not agree with the experimental results. Therefore, we show in Fig. 9 the calculated results for $T_{\mathrm{a}} = 100.1$ and $78.0\,^{\circ}\mathrm{C}$ for PMMA and PVC, respectively, as the examples that show the feature of the dependence of two maxima on the annealing time most remarkably.

Figure 9 shows that $C_{\mathrm{p\,max}}^{\mathrm{L}}$ and $T_{\mathrm{max}}^{\mathrm{L}}$ increase with t_{a} while $C_{\mathrm{p\,max}}^{\mathrm{H}}$ and $T_{\mathrm{max}}^{\mathrm{H}}$ remain unchanged in agreement with the experimental results. Calculation 1 reproduces the dependence of two maxima in specific heat on the annealing time in the enthalpy relaxation. This result indicates that the variation in the relaxation time during annealing is not always necessary for the appearance of two maxima in specific heat.

We discuss the condition under which two maxima in specific heat are observed, and the factor that determines the number of maxima in specific heat under a history of a typical annealing experiment. We will hereafter show the calculated results only for PMMA for discussion.

Figure 9 indicates that the higher maximum nearly agrees with the maximum in the unannealed specific heat, and that the lower maximum is observed only in the case in which the sample undergoes the annealing history. We expect that the lower maximum in specific heat originates from the annealing history, and the higher one originates from the rest of the history, i.e., the cooling and the heating in Fig. 1.

To examine the contribution of the history as shown in Fig. 1 to the maximum in specific heat, the integral in Eq. (1)

at a time $t > t_{\mathrm{HT}}$ during the heating process is decomposed into two components $\delta S_{\mathrm{anneal}}(t)$ and $\delta S'(t)$. These are the contributions to $\delta S(t)$ during annealing and the rest of the history, respectively:

$$\delta S(t) \equiv S(t) - S^{\mathrm{eq}}[T(t)] = \delta S_{\mathrm{anneal}}(t) + \delta S'(t) \quad (9)$$

$$= -\int_0^t \overline{\Delta\chi}[T(t),T(t')][T(t) - T(t')]\frac{\partial\phi[\tilde{t}(t,t')]}{\partial t'}dt'. \quad (10)$$

Since $T(t') = T_{\mathrm{a}} = \mathrm{const}$ for $t_{\mathrm{AN}} \leqslant t' \leqslant t_{\mathrm{CL2}}$, $\delta S_{\mathrm{anneal}}(t)$ is written by

$$\delta S_{\mathrm{anneal}}(t)$$
$$= -\int_{t_{\mathrm{AN}}}^{t_{\mathrm{CL2}}} \overline{\Delta\chi}[T(t),T(t')][T(t) - T(t')]\frac{\partial\phi[\tilde{t}(t,t')]}{\partial t'}dt'$$
$$= -\overline{\Delta\chi}[T(t),T_{\mathrm{a}}][T(t) - T_{\mathrm{a}}]\{\phi[\tilde{t}(t,t_{\mathrm{CL2}})] - \phi[\tilde{t}(t,t_{\mathrm{AN}})]\}, \quad (11)$$

and $\delta S'(t)$ is

$$\delta S'(t) = -\int_0^{t_{\mathrm{AN}}} \overline{\Delta\chi}[T(t),T(t')][T(t) - T(t')]\frac{\partial\phi[\tilde{t}(t,t')]}{\partial t'}dt'$$
$$-\int_{t_{\mathrm{CL2}}}^t \overline{\Delta\chi}[T(t),T(t')][T(t) - T(t')]\frac{\partial\phi[\tilde{t}(t,t')]}{\partial t'}dt'. \quad (12)$$

The thick and thin curves in Fig. 10(a) show $\delta S_{\mathrm{anneal}}(t)$ and $\delta S'(t)$ against temperature in the heating process, respectively. At short t_{a} of $1 \leqslant t_{\mathrm{a}} \leqslant 10^2$ min, $\delta S'(t)$ hardly depends on t_{a}. Therefore, the main contribution to the annealing time dependence of $\delta S(t)$ arises from $\delta S_{\mathrm{anneal}}$. In Eq. (11), $\delta S_{\mathrm{anneal}}(t)$ consists of two factors: a factor $-\overline{\Delta\chi}[T(t),T_{\mathrm{a}}][T(t) - T_{\mathrm{a}}]$, which is the entropy difference arising from the temperature difference between a temperature at the present time, $T(t)$, and T_{a}, and another factor $\phi[\tilde{t}(t,t_{\mathrm{CL2}})] - \phi[\tilde{t}(t,t_{\mathrm{AN}})]$, which represents the amount of relaxation during annealing. The first factor, $-\overline{\Delta\chi}[T(t),T_{\mathrm{a}}][T(t) - T_{\mathrm{a}}]$, decreases monotonically with $T(t)$ passing through zero at $T(t) = T_{\mathrm{a}}$ and is independent of t_{a}, as shown by the black thick curve in Fig. 10(b). The second factor, $\phi[\tilde{t}(t,t_{\mathrm{CL2}})] - \phi[\tilde{t}(t,t_{\mathrm{AN}})]$, is constant at low $T(t)$ in the glassy state since $\tilde{t}(t,t_{\mathrm{CL}})$ and $\tilde{t}(t,t_{\mathrm{AN}})$ do not vary due to very large $\tau(t)$. It begins to decrease in the glass-transition region and approaches zero at high $T(t)$ in the equilibrium liquid state. The factor $\phi[\tilde{t}(t,t_{\mathrm{CL2}})] - \phi[\tilde{t}(t,t_{\mathrm{AN}})]$ increases with t_{a} if T_{a} is fixed as shown by the thin curves in Fig. 10(b). As a result, $\delta S_{\mathrm{anneal}}(t)$, expressed by the product of these factors, decreases at low $T(t)$ in the glassy state, passes through zero at $T(t) = T_{\mathrm{a}}$, and approaches zero again at high $T(t)$. The minimum and the inflection point in $\delta S_{\mathrm{anneal}}(t)$ are between $T(t) = T_{\mathrm{a}}$ and high temperatures. The slope of $\delta S_{\mathrm{anneal}}(t)$ at low $T(t)$ increases with t_{a}. The position of the minimum and the inflection point in $\delta S_{\mathrm{anneal}}(t)$ shift toward high temperatures with t_{a} as shown by the thick curves in Fig. 10(a), when the logarithm of the relaxation function, $\log\phi(t)$, is downward convex, that is, the relaxation time has the distribution and a monotonically decreasing function. Therefore, from the above discussion, $\delta S'(t)$ has an inflection point unchanged independent of t_{a}, while the inflection point

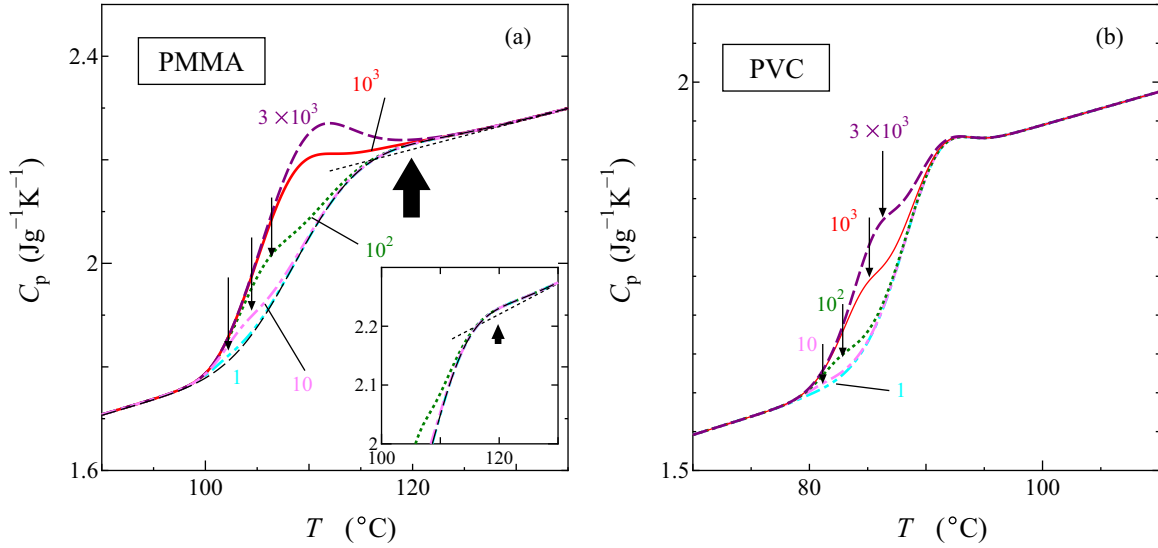FIG. 9. Specific heat calculated by calculation 1 in the heating process after annealing at (a) $T_a = 100.1\,^\circ$C for PMMA and (b) $T_a = 78.0\,^\circ$C for PVC, for t_a in the range from 1 to 3×10^3 min. The line types are the same as Fig. 7(b). The down-arrows represent the lower maxima in specific heat. and the bold up-arrow represents the higher maximum. The black thin dashed curve in (a) shows the unannealed result for PMMA. The black thin dotted line represents the specific heat in the liquid state C_p^0. The inset is a closeup of specific heat in the glass-transition region, where only unannealed results and the results for $t_a = 1$, 10, and 10^2 min are shown. The unannealed results and the results for $t_a = 1$ and 10 min are almost identical to each other in the inset. The numbers in the figure represent the annealing time in minutes.

of $\delta S_{\mathrm{anneal}}(t)$ shifts toward high temperatures and the slope at the inflection point increases with t_a. Note that when the aging effects are small, for example when T_a is low or t_a is short, $\delta S'(t)$ is almost independent of t_a. So it is effective to discuss two maxima by the decomposition of thermal history shown in Fig. 1 into the annealing and the rest of history only when the aging effects are small.

The sum of $\delta S'(t)$ and $\delta S_{\mathrm{anneal}}(t)$ in Fig. 10(a), $\delta S(t)$, is shown for $t_a = 1$, 10, and 10^2 min in Fig. 10(c). The dashed and solid circles in Fig. 10(c) show the inflection points of $\delta S'(t)$ and $\delta S_{\mathrm{anneal}}(t)$, respectively, which correspond to the higher and the lower maxima in $\delta S(t)$. The higher maximum in specific heat, originating from $\delta S'(t)$, are observed above T_g. The lower maximum, originating from $\delta S_{\mathrm{anneal}}(t)$, depends on the annealing condition, and it is observed just above T_a for $t_a \to 0$ and approaches the higher maximum with increasing t_a. We can observe two maxima in specific heat within the experimental accuracy when two maxima originating from two different thermal histories are separated and have measurable magnitude within the experimental accuracy. From the viewpoint of the inflection point in $\delta S(t)$, when the inflection point in $\delta S_{\mathrm{anneal}}(t)$ is located at a temperature low enough not to overlap the inflection point in $\delta S'(t)$, and the slope at the inflection point in $\delta S_{\mathrm{anneal}}(t)$ has the magnitude comparable to that in $\delta S'(t)$, two maxima in specific heat are observed.

For a long annealing time, the minimum in $\delta S_{\mathrm{anneal}}(t)$ becomes small and the position of the minimum shifts to a high temperature due to an increase in $\phi[\tilde{t}(t,t_{\mathrm{CL2}})] - \phi[\tilde{t}(t,t_{\mathrm{AN}})]$. As a consequence, the minimum, or the inflection point in $\delta S_{\mathrm{anneal}}(t)$, overlaps with that in $\delta S'(t)$, and $\delta S(t)$ has only one inflection point. For high annealing temperature, $\delta S(t)$ has only one inflection point due to the overlap of $\delta S_{\mathrm{anneal}}(t)$ with $\delta S'(t)$.

For a low annealing temperature, the magnitude of the minimum in $\delta S_{\mathrm{anneal}}(t)$ becomes small comparable to that in $\delta S'(t)$ due to small $\phi[\tilde{t}(t,t_{\mathrm{CL2}})] - \phi[\tilde{t}(t,t_{\mathrm{AN}})]$. So $\delta S(t)$ apparently has only one inflection point originating from $\delta S'(t)$. For a short annealing time for the same reason, $\delta S(t)$ has only one inflection point from $\delta S'(t)$. In these cases, the minimum in $\delta S_{\mathrm{anneal}}(t)$ actually exists between T_a and the higher maximum, but its magnitude is just too small to measure within the experimental accuracy.

From the discussion above, two factors determine the number of maxima in specific heat. One is an annealing temperature, which determines the position of the lower maximum for $t_a \to 0$. An annealing temperature sufficiently lower than T_g allows the separation between $\delta S_{\mathrm{anneal}}(t)$ and $\delta S'(t)$ and prevents $\delta S_{\mathrm{anneal}}(t)$ from overlapping with $\delta S'(t)$. The other is the amount of relaxation during annealing, $\phi[\tilde{t}(t,t_{\mathrm{CL2}})] - \phi[\tilde{t}(t,t_{\mathrm{AN}})]$, which determines the position and the magnitude of the lower maximum for a finite t_a. When $\phi[\tilde{t}(t,t_{\mathrm{CL2}})] - \phi[\tilde{t}(t,t_{\mathrm{AN}})]$ is not too large, that is, the aging effect is not too large, the lower maximum is located between T_a and the higher one without overlapping with the higher one, and if the aging effect is too small, the lower one cannot be observed within the experimental accuracy. A gradual change in $\phi[\tilde{t}(t,t_{\mathrm{CL2}})] - \phi[\tilde{t}(t,t_{\mathrm{AN}})]$ with t_a dependent on the decay of the relaxation function leads to a broad range of t_a over which $\phi[\tilde{t}(t,t_{\mathrm{CL2}})] - \phi[\tilde{t}(t,t_{\mathrm{AN}})]$ does not become too large. In the case of the KWW function, used as an approximation of the relaxation function in this study, the exponent β, i.e., the width of the distribution of the relaxation time, determines how gradually the relaxation function decays if T_a is fixed. The broad distribution of the relaxation time, that is, small β, leads to the gradual decay of the relaxation function, which allows us to observe two maxima under typical annealing conditions.
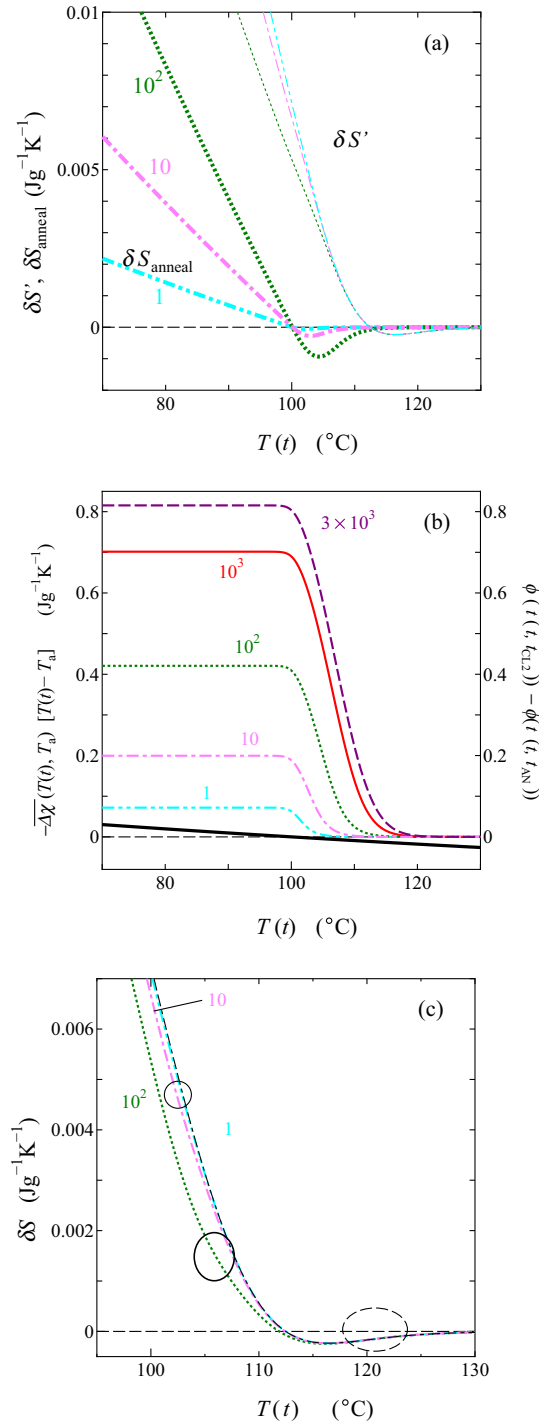
FIG. 10. Temperature dependence of (a) $\delta S_{anneal}(t)$ (bold) and $\delta S'(t)$ (thin), (b) $-\overline{\Delta\chi}[T(t),T_a][T(t)-T_a]$ (black bold) and $\phi[\tilde{t}(t,t_{CL2})]-\phi[\tilde{t}(t,t_{AN})]$ (colored thin curves), and (c) $\delta S(t)$, the sum of $\delta S'(t)$ and $\delta S_{anneal}(t)$ in (a), for $T_a=100.1\,^{\circ}\mathrm{C}$ in the heating process by calculation 1. The dotted, dashed-dotted, dashed-two dotted, solid, and dashed curves represent $t_a=1,10$, and 10^2, 10^3, and 3×10^3 min, respectively. The numbers in the figure represent t_a in minutes. For the comparison, unannealed $\delta S(t)$ is also shown by the black two dashed-dotted curves in (c). The higher inflection point in $\delta S(t)$ and the ones in δS_{anneal} against temperature are shown by the solid and the dashed circles in (c), respectively.

E. Results by calculations 2 and 3

So far we have discussed the appearance of two maxima in specific heat qualitatively based on calculation 1. Calculation 1 can reproduce two maxima in specific heat qualitatively. However, the results by calculation 1 do not show a quantitative agreement with the experimental results. In this subsection, we introduce calculations 2 and 3, and we discuss the quantitative agreement with the experimental results.

The results obtained by calculation 2 are shown by thin curves in Figs. 7(b) and 7(c). Figures 7(b) and 7(c) show that calculation 2 reproduces two maxima in specific heat and their annealing condition dependence qualitatively, but the quantitative agreement with the experimental results is not sufficient. So we introduce calculation 3 for a quantitative agreement with the experimental results by reestimating the configurational entropy that determines the relaxation time.

In calculation 3, the parameters $\Delta\chi_F$, σ_F, and T_F are determined by the trial and error method so that the upper limit of annealing temperature where two maxima are observed agrees with that of experimental results for $t_a=10^2,10^3$, and 3×10^3 min for PMMA, and for $t_a=10^2$ and 10^3 min for PVC. We have obtained $\Delta\chi_F=-6.5\times10^{-5}\,\mathrm{J\,g^{-1}\,K^{-2}}$, $\sigma_F=35$ K, and $T_F=346$ K for PMMA, and $\Delta\chi_F=-1.40\times10^{-4}\,\mathrm{J\,g^{-1}\,K^{-2}}$, $\sigma_F=23$ K, and $T_F=353$ K for PVC. The least-squares fitting to the experimental relaxation time by Eq. (4) with these sets of the parameters gives $\tau_\infty^{(3)}=1.69\times10^{-4}$ s, $A^{(3)}=104\,\mathrm{J\,g^{-1}\,K^{-2}}$, and $T_2^{(3)}=359$ K for PMMA, $\tau_\infty^{(3)}=4.08\times10^{-12}$ s, $A^{(3)}=343\,\mathrm{J\,g^{-1}\,K^{-2}}$, and $T_2^{(3)}=324$ K for PVC. The fitting curve thus obtained for PVC is shown in Fig. 4 by the dotted curve and hardly differs from $\tau(T)$ in the temperature range shown in Fig. 4.

The results obtained by calculation 3 are shown in Figs. 7(b), 7(c), and 8. The quantitative agreement with the experimental results is improved from calculation 2. Figure 7 shows that in calculation 3, the lower maximum in specific heat is observed for $t_a=10^3$ and 3×10^3 min in agreement with the experimental results. Figure 8 shows that for the short annealing time and the high annealing temperature, the results obtained by calculation 3 agree with the experimental ones quantitatively.

Finally we comment on the possibility of two maxima in specific heat in PS. In the enthalpy relaxation in PS, only one maximum is usually observed. We have shown above that the observation of two maxima needs the separation of two contributions from the two thermal histories, that is, annealing and the rest of the history, $\delta S_{anneal}(t)$ and $\delta S'(t)$. In polystyrene, these two contributions overlap with each other under typical annealing conditions such as the annealing just below T_g, so that only one maximum is observed. We expect that if the annealing temperature is low enough to separate these two contributions sufficiently, and the annealing time is long enough for the contribution of the annealing, $\delta S_{anneal}(t)$ to be observed within the experimental accuracy, two maxima in specific heat will be observed in PS. This experiment is in progress and the results will be reported in the near future.

V. CONCLUSIONS

The dependence of enthalpy relaxation in PMMA and PVC on annealing conditions has been studied by DSC and using the calculation by the phenomenological model equation, with the parameters obtained experimentally. Two specific-heat maxima have been observed at higher and lower temperatures in the glass-transition region. The higher maximum is observed above T_g; the lower maximum is observed above T_a and shifts toward the higher maximum with increasing t_a. The calculation in which only one relaxation is taken into account, and the relaxation time is that in equilibrium and does not vary during annealing, has reproduced two maxima in specific heat. This result indicates that the appearance of two maxima in specific heat is not always necessary for two relaxations and for an increase in the relaxation time during annealing. The analysis based on the calculation has clarified the origin of two maxima in the enthalpy relaxation; the higher maximum originates from the history except for the annealing, that is, cooling and heating, and the lower one originates from the annealing history. The position and the magnitude of the lower maximum are determined by T_a and the intensity of the aging, that is, how the relaxation toward the equilibrium state proceeds; as the annealing temperature becomes higher, or the aging becomes heavier, the lower maximum shifts toward higher temperatures and consequently merges the higher maximum. The number of maxima in specific heat, either one or two, is determined by an annealing temperature and how the relaxation function decays. In the present analysis, the width of the relaxation time distribution, i.e., the value of β, plays a major role in the determination of the number of maxima in the specific heat.

[1] A. Q. Tool, J. Am. Ceram. Soc. **29**, 240 (1946).

[2] O. S. Narayanaswamy, J. Am. Ceram. Soc. **54**, 491 (1971).

[3] C. T. Moynihan, A. J. Easteal, M. A. DeBolt, and J. Tucker, J. Am. Ceram. Soc. **59**, 12 (1976).

[4] A. J. Kovacs, J. J. Aklonis, J. M. Hutchinson, and A. R. Ramos, J. Polym. Sci., Phys. Ed. **17**, 1097 (1979).

[5] J. L. Gómez Ribelles and M. Monleón Pradas, Macromolecules **28**, 5867 (1995).

[6] V. M. Boucher, D. Cangialosi, A. Alegría, and J. Colmenero, Macromolecules **44**, 8333 (2011).

[7] R. Golovchar, A. Kozdras, V. Balitska, and O. Shpotyuk, J. Phys.: Condens. Matter **24**, 505106 (2012).

[8] D. Cangialosi, V. M. Boucher, A. Alegría, and J. Colmenero, Phys. Rev. Lett. **111**, 095701 (2013).

[9] G. Liu, Y. Zuo, D. Zhao, and M. Zhang, J. Non-Cryst. Solids **402**, 160 (2014).

[10] R. S. Miller and R. A. MacPhail, J. Chem. Phys. **106**, 3393 (1997).

[11] Y. P. Koh and S. L. Simon, Macromolecules **46**, 5815 (2013).

[12] W. Sakatsuji, T. Konishi, and Y. Miyamoto, Phys. Rev. E **88**, 012605 (2013).

[13] Y. Miyamoto, K. Fukao, H. Yamao, and K. Sekimoto, Phys. Rev. Lett. **88**, 225504 (2002).

[14] I. M. Hodge, Macromolecules **16**, 898 (1983).

[15] I. M. Hodge, Macromolecules **20**, 2897 (1987).

[16] A. R. Berens and I. M. Hodge, Macromolecules **15**, 756 (1982).

[17] A. R. Berens and I. M. Hodge, Polym. Eng. Sci. **24**, 1123 (1984).

[18] W. Sakatsuji, T. Konishi, and Y. Miyamoto, J. Therm. Anal. Calorim. **113**, 1129 (2013).

[19] R. Bergman, F. Alvarez, A. Alegría, and J. Colmenero, J. Chem. Phys. **109**, 7546 (1998).

[20] R. Bergman, F. Alvarez, A. Alegría, and J. Colmenero, J. Non-Cryst. Solids **235-237**, 580 (1998).

[21] E. Muzeau, J. Perez, and G. P. Johari, Macromolecules **24**, 4713 (1991).

[22] J. Colmenero, A. Arbe, and A. Alegría, Physica A **201**, 447 (1993).

[23] R. Flores and J. Perez, Macromolecules **28**, 7171 (1995).

[24] E. Hempel, M. Beiner, H. Huth, and E. Donth, Thermochim. Acta **391**, 219 (2002).

[25] G. Adam and J. H. Gibbs, J. Chem. Phys. **43**, 139 (1965).

[26] I. M. Hodge, Macromolecules **19**, 936 (1986).

[27] J. M. Hutchinson, S. Montserrat, Y. Calventus, and P. Cortés, J. Non-Cryst. Solids **307-310**, 412 (2002).

[28] J. W. P. Schmelzer and I. S. Gutzow, *Generic Theory of Vitrification of Glass-Forming Melts* (Wiley-VCH, Weinheim, 2011), Chap. 3.

[29] E. Tombari and G. Johari, J. Chem. Phys. **141**, 074502 (2014).

[30] G. Williams and D. C. Watts, Trans. Faraday Soc. **66**, 80 (1970).

[31] J. Colmenero, A. Alegría, A. Arbe, and B. Frick, Phys. Rev. Lett. **69**, 478 (1992).

[32] T. Odagaki, T. Yoshidome, A. Koyama, and A. Yoshimori, J. Non-Cryst. Solids **352**, 4843 (2006).

[33] T. Odagaki and A. Yoshimori, J. Non-Cryst. Solids **355**, 681 (2009).

[34] A. Yoshimori and T. Odagaki, J. Phys. Soc. Jpn. **80**, 064601 (2011).